AFRL-DE-PS-
TR-2005-1043

A CONICAL SLOT ANTENNA AND RELATED ANTENNAS SUITABLE FOR USE WITH AN AIRCRAFT WITH INFLATABLE WINGS

Everett G. Farr
W. Scott Bigelow

Farr Research, Inc.
614 Paseo Del Mar NE
Albuquerque, NM 87123

23 February 2005

Final Report

APPROVED FOR PUBLIC RELEASE; DISTRIBUTION IS UNLIMITED.

AIR FORCE RESEARCH LABORATORY
Directed Energy Directorate
3550 Aberdeen Ave SE
AIR FORCE MATERIEL COMMAND
KIRTLAND AIR FORCE BASE, NM 87117-5776

STINFO COPY

AFRL-DE-PS-TR-2005-1043

This report has been approved for publication.

//SIGNED//
JOSEPH L. BROECKERT, 2d Lt, USAF
Project Manager

//SIGNED//
THOMAS A. SPENCER, DR-IV
Acting Chief, High Power Microwave Division

//SIGNED//
L. BRUCE SIMPSON, SES
Director, Directed Energy Directorate

REPORT DOCUMENTATION PAGE

Form Approved
OMB No. 0704-0188

1. REPORT DATE *(DD-MM-YYYY)*	2. REPORT TYPE	3. DATES COVERED *(From - To)*
23 February 2005	Final Report	May 2004 – Feb 2005

4. TITLE AND SUBTITLE
A Conical Slot Antenna and Related Antennas Suitable for Use with an Aircraft with Inflatable Wings

5a. CONTRACT NUMBER
FA9451-04-M-0080

5b. GRANT NUMBER
N/A

5c. PROGRAM ELEMENT NUMBER
65502F

6. AUTHOR(S)
Everett G. Farr and W. Scott Bigelow

5d. PROJECT NUMBER
3005

5e. TASK NUMBER
DP

5f. WORK UNIT NUMBER
DH

7. PERFORMING ORGANIZATION NAME(S) AND ADDRESS(ES)

Farr Research, Inc.
614 Paseo Del Mar NE
Albuquerque, NM 87123

8. PERFORMING ORGANIZATION REPORT NUMBER

9. SPONSORING / MONITORING AGENCY NAME(S) AND ADDRESS(ES)

Air Force Research Laboratory
3550 Aberdeen Avenue SE
Kirtland AFB NM 87117-5776

10. SPONSOR/MONITOR'S ACRONYM(S)
AFRL/DEHP

11. SPONSOR/MONITOR'S REPORT NUMBER(S)
AFRL-DE-PS-TR-2005-1043

12. DISTRIBUTION / AVAILABILITY STATEMENT
APPROVED FOR PUBLIC RELEASE; DISTRIBUTION IS UNLIMITED.

13. SUPPLEMENTARY NOTES

14. ABSTRACT

Airborne UWB radar systems require receive antennas that can be printed or mounted onto an inflatable wing. Such antennas need to reach as low as VHF frequencies, and must be positioned to look to the side of the aircraft. To satisfy these requirements, a tapered slot antenna (TSA) looking off the wingtip has been proposed. However, a conventional TSA receives only horizontal polarization. Here, we describe a new form of TSA, the conical slot antenna (CSA), which exhibits vertical polarity above and below the horizon. To test the approach, we built and tested a 1/8th scale model of a CSA. We observed a clean impulse response with FWHM of less than 70 ps. The maximum gain for both polarizations is between 0 and 10 dBi from 4 to 12 GHz. The return loss, however, is higher than we would like over most of the frequency range. Finally, we discuss a number of alternative concepts for mounting antennas onto UAVs with inflatable wings.

15. SUBJECT TERMS
Tapered Slot Antenna, Conical Slot Antenna Vivaldi Antenna, Ultra-Wideband (UWB) radar, Unmanned Aerial Vehicle, Time Domain Antenna Range

16. SECURITY CLASSIFICATION OF:			17. LIMITATION OF ABSTRACT	18. NUMBER OF PAGES	19a. NAME OF RESPONSIBLE PERSON
a. REPORT	b. ABSTRACT	c. THIS PAGE			Joseph Broeckert
Unclassified	Unclassified	Unclassified	SAR	28	19b. TELEPHONE NUMBER *(include area code)* (505)853-4707

Standard Form 298 (Rev. 8-98)
Prescribed by ANSI Std. 239.18

(This page is intentionally left blank)

CONTENTS

FIGURES

1. Introduction

Airborne ultra wideband (UWB) radar systems require receive antennas that can be printed or mounted onto an inflatable wing. Examples of inflatable wings are shown in [1]. Antennas are needed that can reach as low as VHF frequencies and must be positioned to look to the side of the aircraft.

To satisfy these requirements a tapered slot antenna (TSA) looking off the wingtip has been proposed. However, a conventional TSA receives only a horizontal polarization and it can not easily be configured to receive vertical polarization. It is well known that polarization diversity can add extra capability to radar, so we explore here how one might add a capability to include a second polarization. In another related effort, we have characterized TSAs, and that work will appear in a forthcoming note.

To add the capability to receive vertical polarization, we propose using a conical slot antenna (CSA) which exhibits vertical polarity above and below the horizon. This antenna was first suggested by C. E. Baum in [2] as a limited-angle-of-incidence and limited-time magnetic sensor, but the concept should be applicable here as well.

To test the approach we built and tested a 1/8th scale model of a CSA. We intended to design for a "typical" wing dimension of 1.52 m (5 ft.) in length by 0.91 m (2 ft.) in width, and our model was 1/8th this size. We observed a clean impulse response with FWHM of less than 70 ps. The maximum gain for both polarizations is between 0 and 10 dBi from 4 to 12 GHz. The return loss, however, is higher than we would like over most of the frequency range.

We begin with a description of the CSA, including its design principles. We then provide measurements of its return loss and antenna pattern. Finally, we discuss a number of alternative concepts for mounting antennas onto unmanned aerial vehicles (UAVs) with inflatable wings.

2. Scale Model UWB Conical Slot Antenna (CSA)

In this project we developed a basic design for a 1/8th scale model of a vertically polarized CSA suitable for application to the underside of an inflatable UAV wing. This class of antenna provides for vertical polarization below the wing, rather than off the wingtip. We built our model from copper foil tape applied to 5 mil Mylar® sheet stock. The antenna was supported by an oversized acrylic frame and was fed by rigid 50 ? coax fitted with a SMA connector as shown in Figure 1. The shield of the coax is soldered to the ground plane adjacent

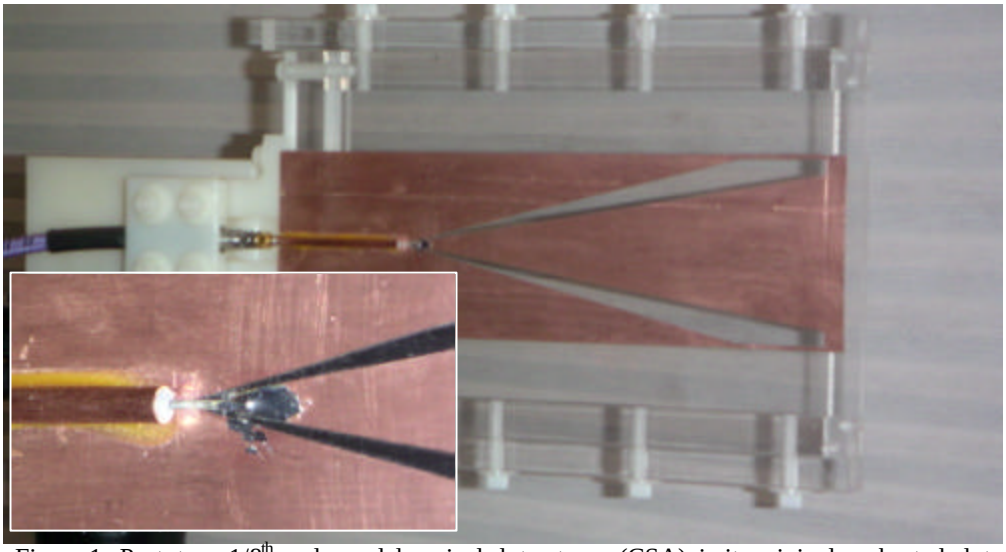

Figure 1. Prototype 1/8th scale model conical slot antenna (CSA), in its original or shorted-slot configuration.

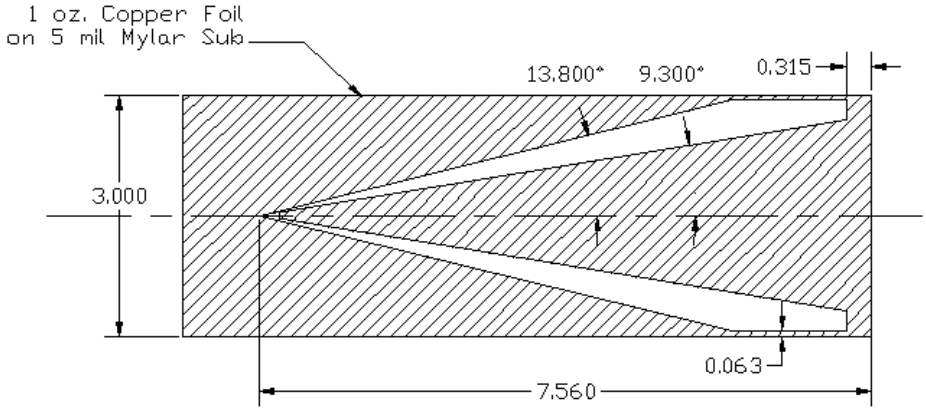

Figure 2. TDR measurements for three configurations of the CSA.

to the apex of the two slots. The cable center conductor bridges the apex gap and is soldered to the truncated tip of the triangular ground plane section. Dimensioning is shown Figure 2.

The CSA design was based on a concept recently suggested by Baum in [2], where he shows that the impedance of the (bent) conical slot and of its dual or complementary structure, the bent biconical coplanar plate antenna, are related as

$$Z_2 = Z_0^2 / 4Z_1 \tag{1}$$

where Z_0 is the impedance of free space, Z_1 is the impedance of the slot and Z_2 is the impedance of the complementary antenna. The latter is like a pair of IRA feed arms, and we find the angles that determine its impedance by using a stereographic projection onto the aperture plane as in [3 and 4]. Although we had wanted to use a slot impedance of 50 ? in order to have a smooth transition from the coaxial feed, the corresponding angular slot width for our geometry was so small (about 1/3-degree) that it would have been impossible to maintain adequate tolerances in our foil tape model. At our chosen 100 ? , the corresponding 4.5 degree slot width is easier to build.

3. Time Domain Reflectometry (TDR) and Return Loss (S_{11}) for the CSA

TDR measurements were made for three configurations of the CSA, distinguished by conditions at the aperture end of the slots: (1) shorted, (2) open, and (3) terminated with a ~100 Ω impedance (220 Ω across each slot), which provides an approximately matched load. The resulting data is displayed in Figure 3, where we note that the data sets overlay at the 50 ? feed line and throughout the nominally 100 ? slot geometry. They diverge at the aperture end of the slots. The corresponding S_{11} data are presented in Figure 4.

On the basis of the TDR data, it would be useful to refine the details of the design at the apex to smooth the transition from the 50 ? coax feed to the 100 ? conical slots. For the original, shorted-slot configuration, the impedance collapse occurs where the slot arms are truncated by the narrow grounded strips at the edge of the antenna structure. From there the impedance continues to decrease until it reverses near the slot ends. The return loss is large (S_{11} exceeds -5 dB) across most of the frequency band.

The CSA configuration represented an approximation of the ideal bent biconical slot magnetic sensor concept introduced by Baum [2]. Because the corresponding return loss was so high we decided to experiment by removing the conductive foil at the slot ends producing the open configuration shown in the photograph of Figure 5. This led to a marginal improvement in S_{11}, primarily at frequencies below about 1 GHz. Later, after preliminary measurements of the impulse response of the CSA were made, we tried terminating the slots at approximately 100 ? with a pair of 220 Ω resistors. This led to a further reduction in return loss at low frequencies. However, since the improvement was minimal the terminating resistors were removed returning the CSA to the open configuration prior subsequent response measurements.

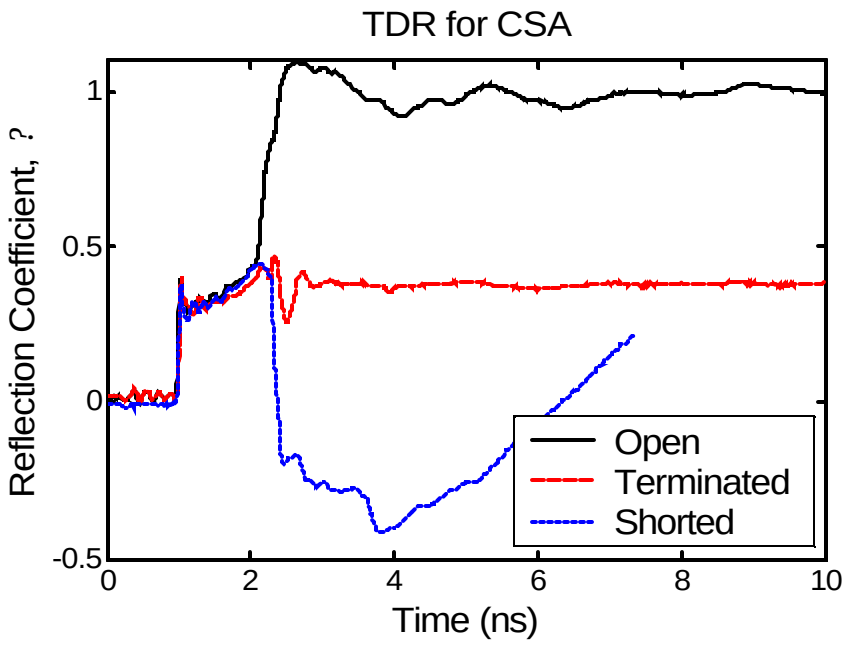

Figure 3. TDR measurements for three configurations of the CSA.

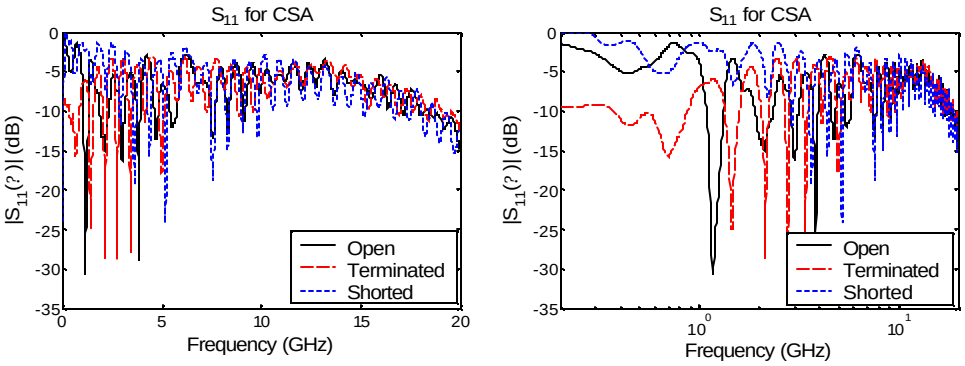

Figure 4. Return loss measurements for three configurations of the CSA ; (a) linear scale, (b) log scale.

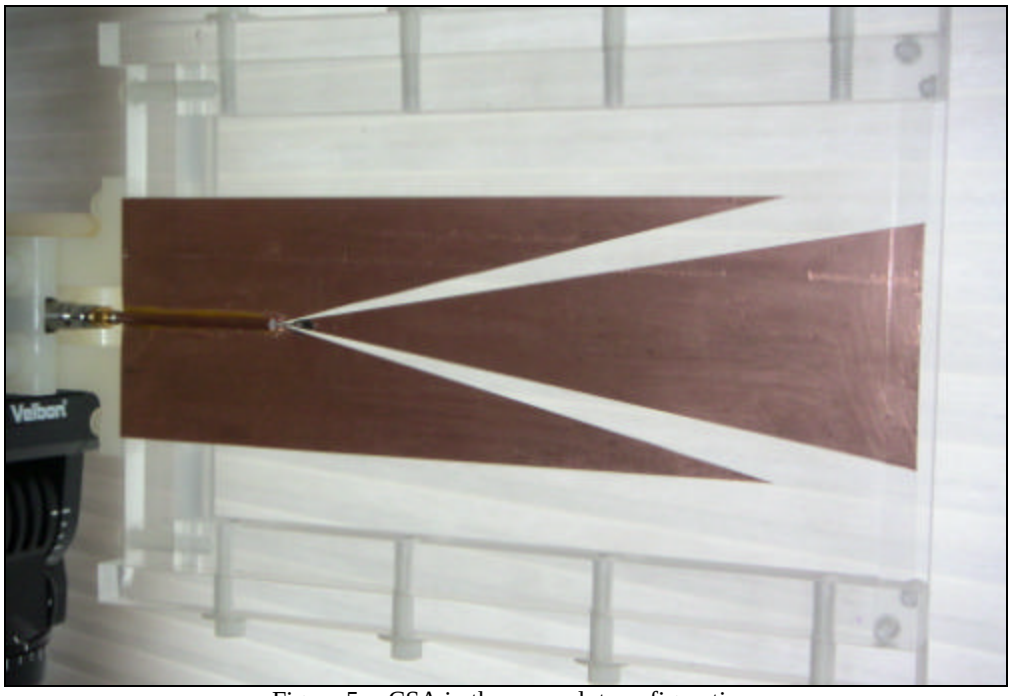

Figure 5. CSA in the open-slot configuration.

4. Impulse Response Measurements

4.1 Preliminary Response Measurements

Our preliminary measurements of the impulse response behavior of the CSA were obtained on the *PATAR*® outdoor antenna range. This range includes a Picosecond Pulse Labs model 4015C step generator, a Tektronix model TDS8000 oscilloscope, and Farr Research model TEM-1-50 sensor and customized elevation/azimuth positioner and software. Subsequently, a more extensive set of measurements was obtained on our indoor range. We began our preliminary measurements by finding that the maximum response of the CSA to vertically polarized (normal to the plane of the antenna, or q) illumination occurs at zero degrees of azimuth and 17 degrees below the horizon (physical boresight). There we recorded the impulse response in the time domain and calculated the corresponding realized gain, as shown in Figure 6. We observe a clean impulse with a FWHM of 47 ps. The peak realized gain of about 8 dB occurs at 8.3 GHz. The frequency range over which the realized gain is above 0 dB is approximately 4 – 12 GHz. Since ours is a 1/8th scale model, at full scale this frequency range corresponds to 0.5 – 1.5 GHz.

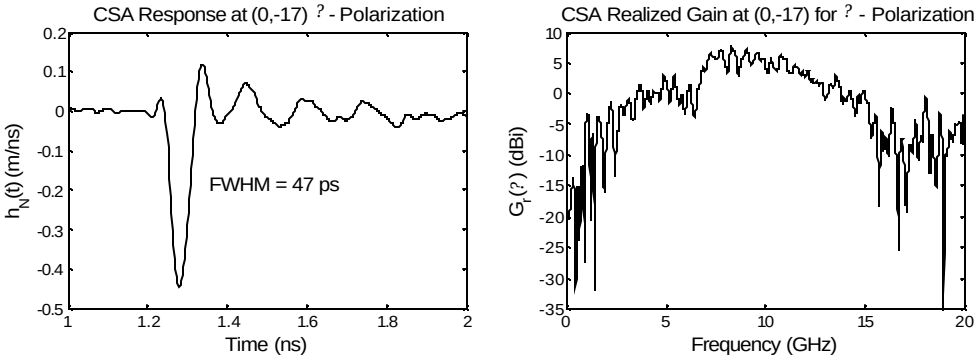

Figure 6. Normalized impulse response and realized gain of the open-slot CSA, at zero degrees of azimuth and -17 degrees of elevation, with vertically polarized (q) illumination.

4.2 Response Pattern Measurements

The CSA was originally conceived as a limited-angle-of-incidence, limited-time magnetic sensor for use in detecting the vertically (q) polarized electric field component scattered from a ground target. However, when the shorting strips were removed from the ends of the CSA slots producing the open-slot configuration, the characteristics of the antenna were dramatically altered. Specifically, the antenna gained sensitivity to the horizontally (f) polarized electric field incident within the plane of the antenna (zero degrees of elevation) from directions off the end of each slot. The dual nature of the open-slot CSA motivated our characterization of the antenna pattern in certain key illumination planes for both horizontal and vertical polarizations.

To characterize the CSA antenna we have made pattern measurements on our indoor range by scanning, with both illumination polarizations, elevations from zero to -45 degrees at zero and -15 degrees of azimuth, and azimuths from zero to -45 degrees at zero and -15 degrees of elevation. The corresponding positive legs of these scans are available by symmetry. In the following sets of figures we present both the pattern data and measurement data at individual key orientation coordinates. The key coordinates are those where relative sensitivity maxima occur, specifically at (AZ,EL) = (f,q) = (0,-15), (-15,0), and (-15,-15).

We begin our characterization of the CSA by examining patterns for the peak normalized impulse response observed in the four planes, AZ = 0, AZ = –15, EL = 0, and EL = –15 degrees, as displayed in Figure 7. Corresponding patterns for realized gain as a function of frequency and angle are shown in Figure 8 and Figure 9. In examining the response data, we see that the vertical polarization component is null at zero degrees elevation, reaching a maximum at (0,-15). The horizontal component is null at zero degrees azimuth, reaching a maximum at (-15,0). At (-15,-15), while not at a maximum, the CSA is about equally sensitive to both polarization components. Physical boresight, (0,0), is a relative null for both components.

In Figure 10 and Figure 11, Figure 12 and Figure 13, and Figure 14 and Figure 15, we present data sets for the three key orientations identified above. Each set includes time domain response and realized gain for both vertical and horizontal polarizations.

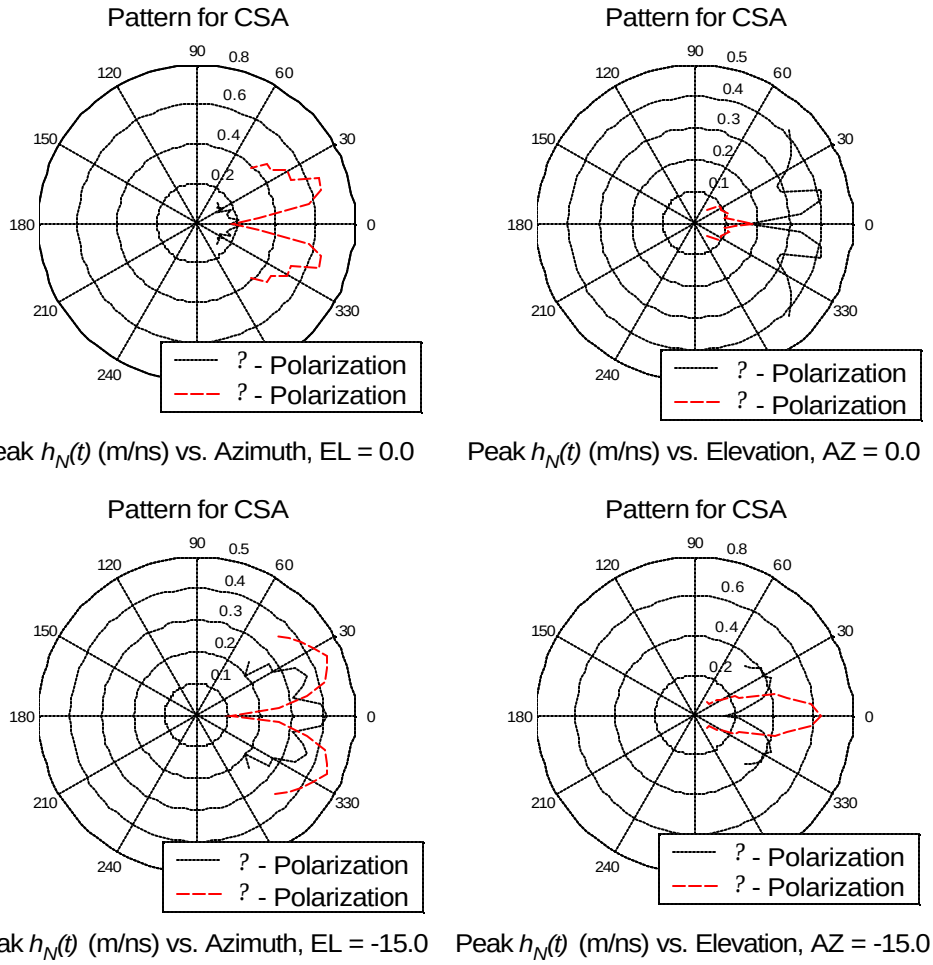

Peak $h_N(t)$ (m/ns) vs. Azimuth, EL = 0.0

Peak $h_N(t)$ (m/ns) vs. Elevation, AZ = 0.0

Peak $h_N(t)$ (m/ns) vs. Azimuth, EL = -15.0

Peak $h_N(t)$ (m/ns) vs. Elevation, AZ = -15.0

Figure 7. Patterns for the peak normalized impulse response of the open-slot CSA.

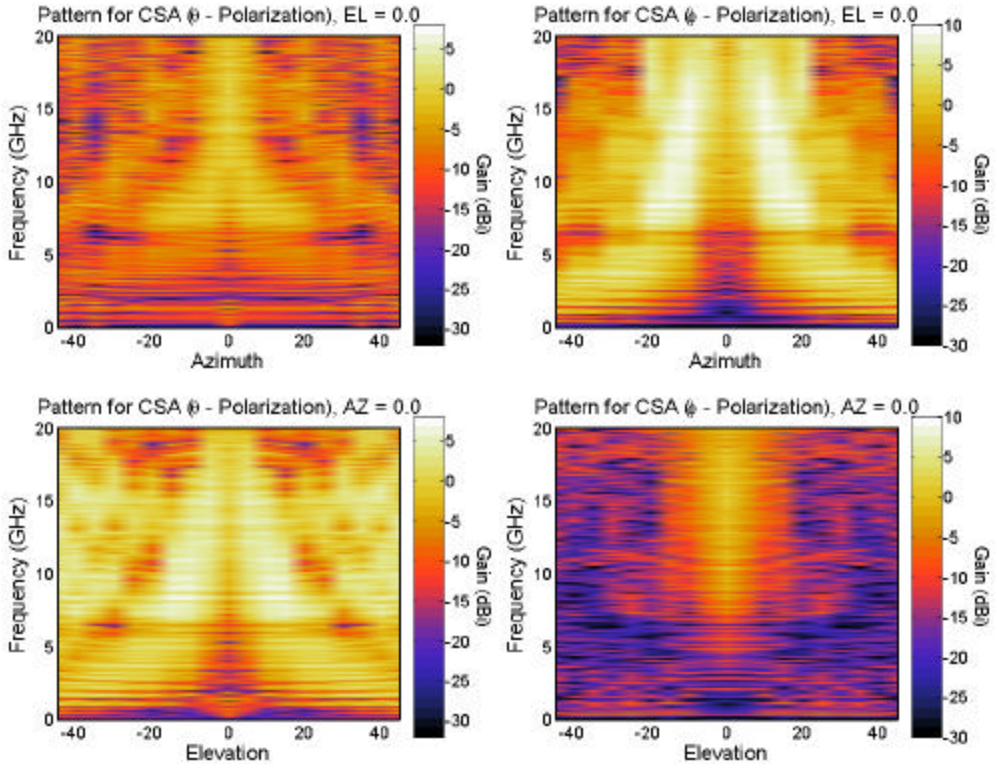

Figure 8. Patterns for the realized gain of the open-slot CSA for EL = 0 and AZ = 0 planes.

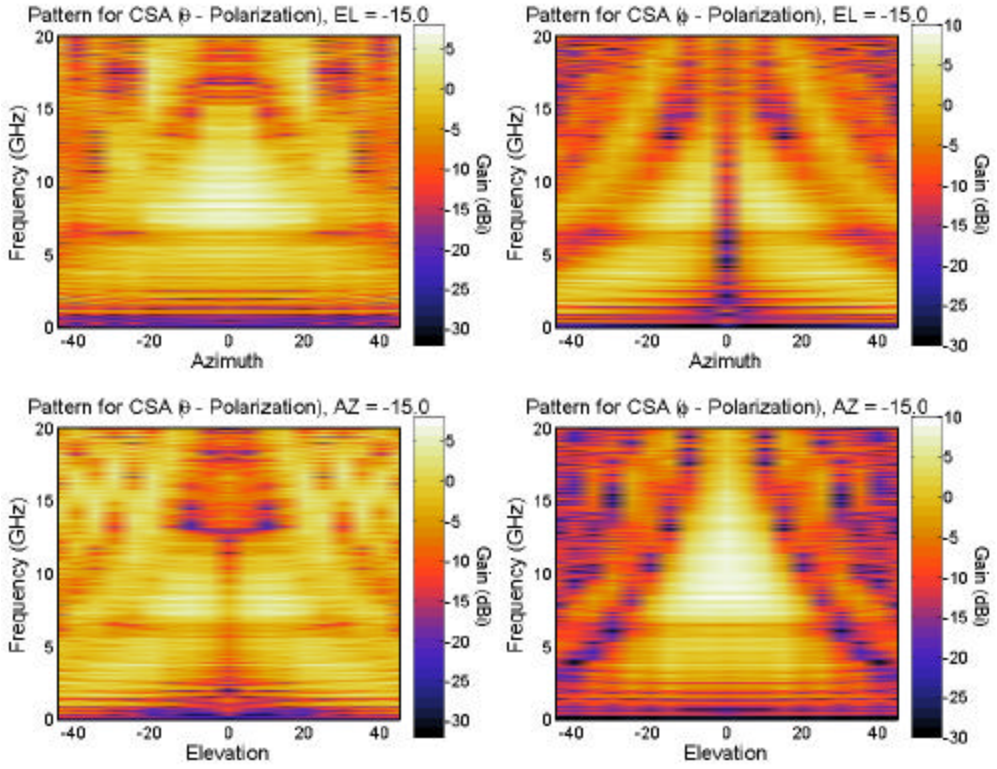

Figure 9. Patterns for the realized gain of the open-slot CSA for EL = 0 and AZ = 0 planes.

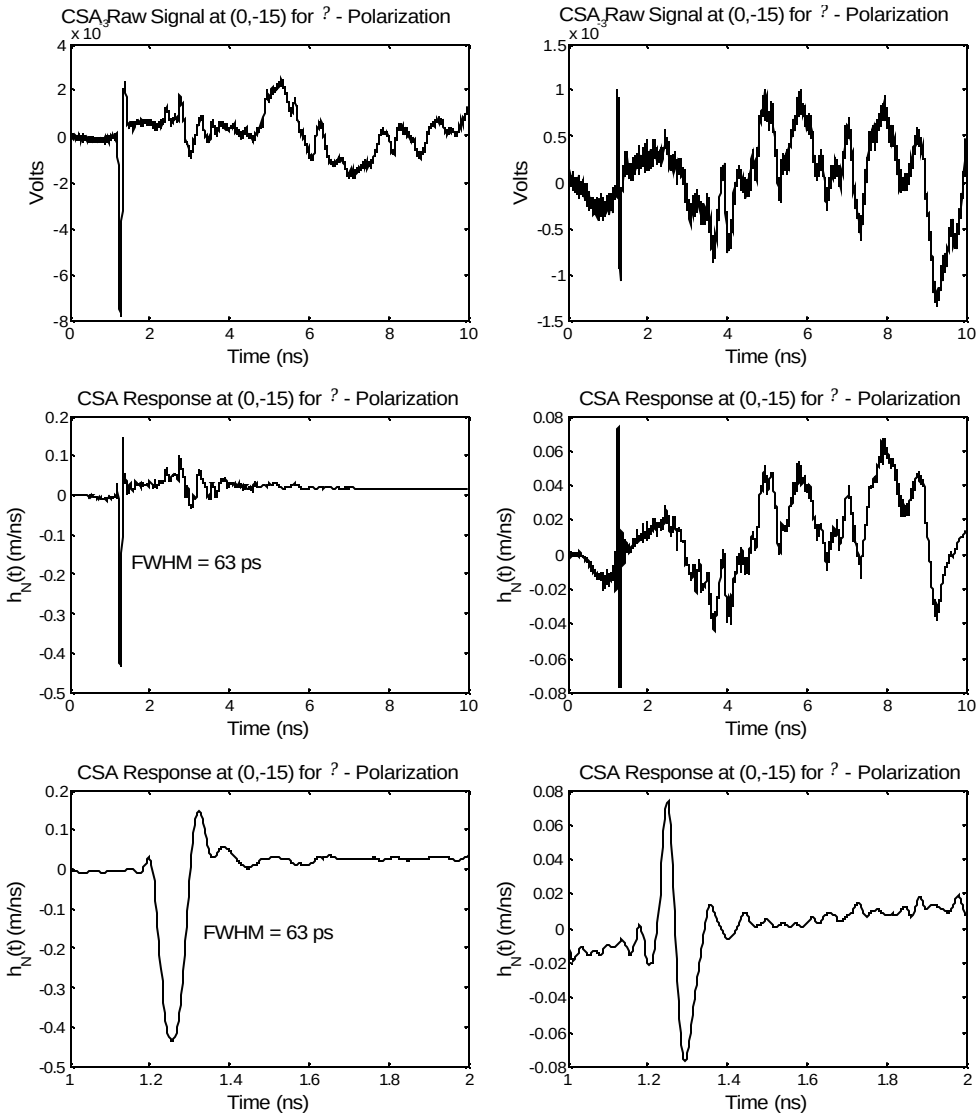

Figure 10. Impulse response of the open-slot CSA at orientation (0,−15).

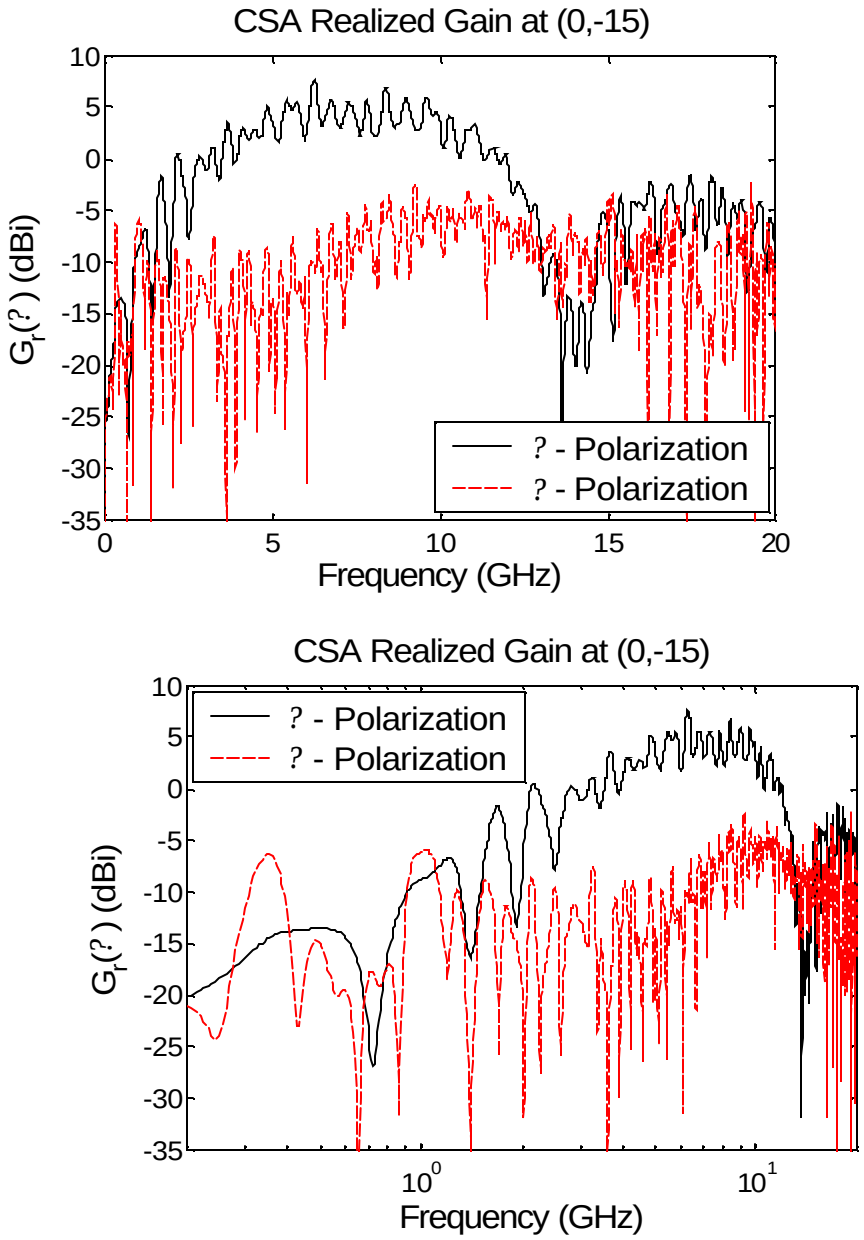

Figure 11. Realized gain of the open-slot CSA at orientation (0,−15).

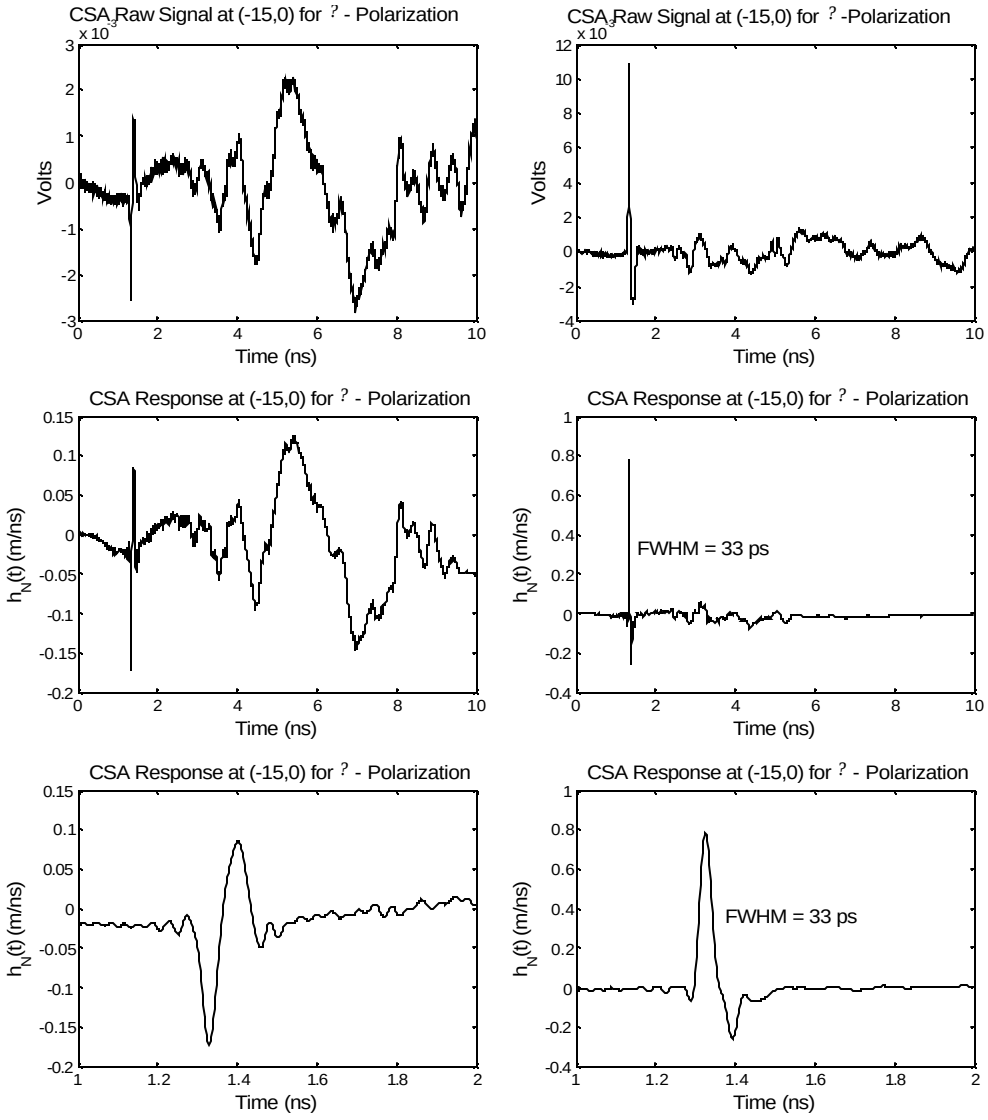

Figure 12. Impulse response of the open-slot CSA at orientation (−15,0).

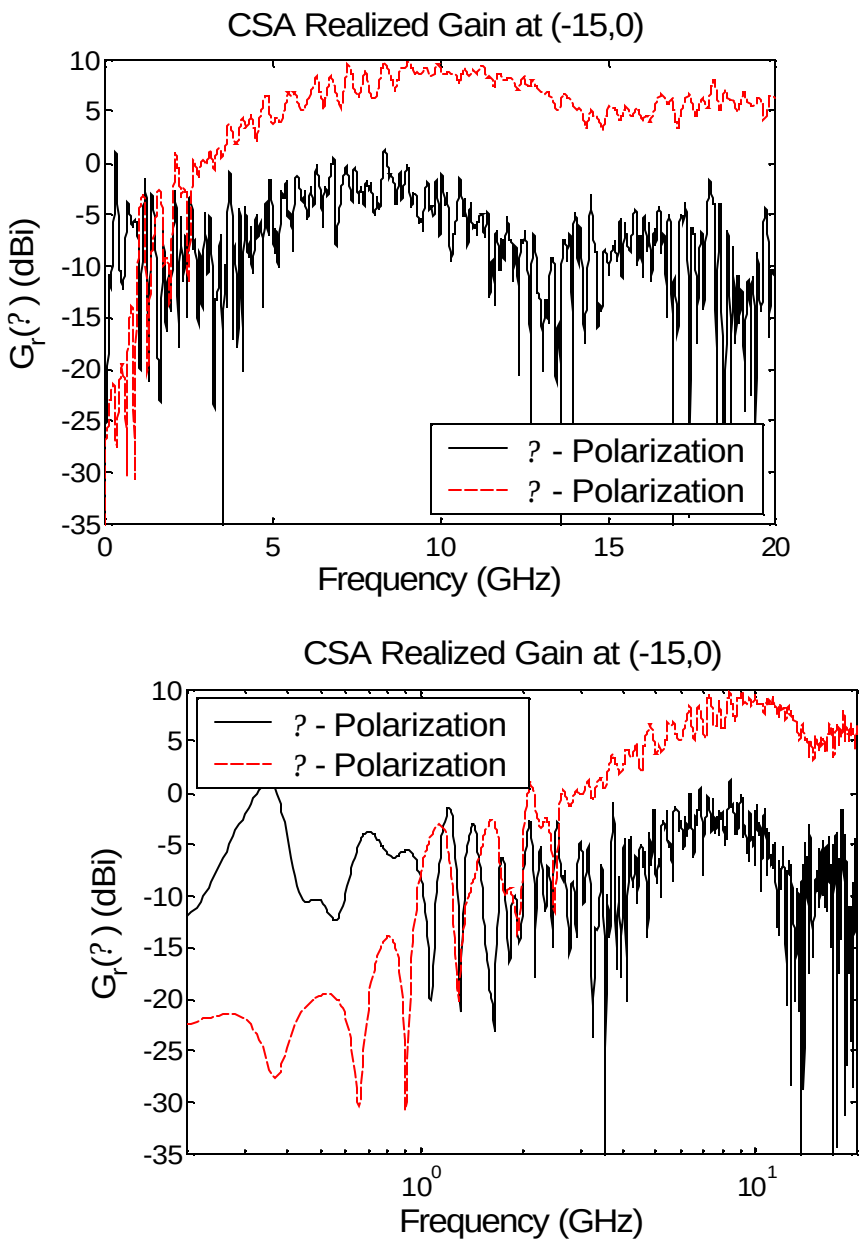

Figure 13. Realized gain of the open-slot CSA at orientation (−15,0)

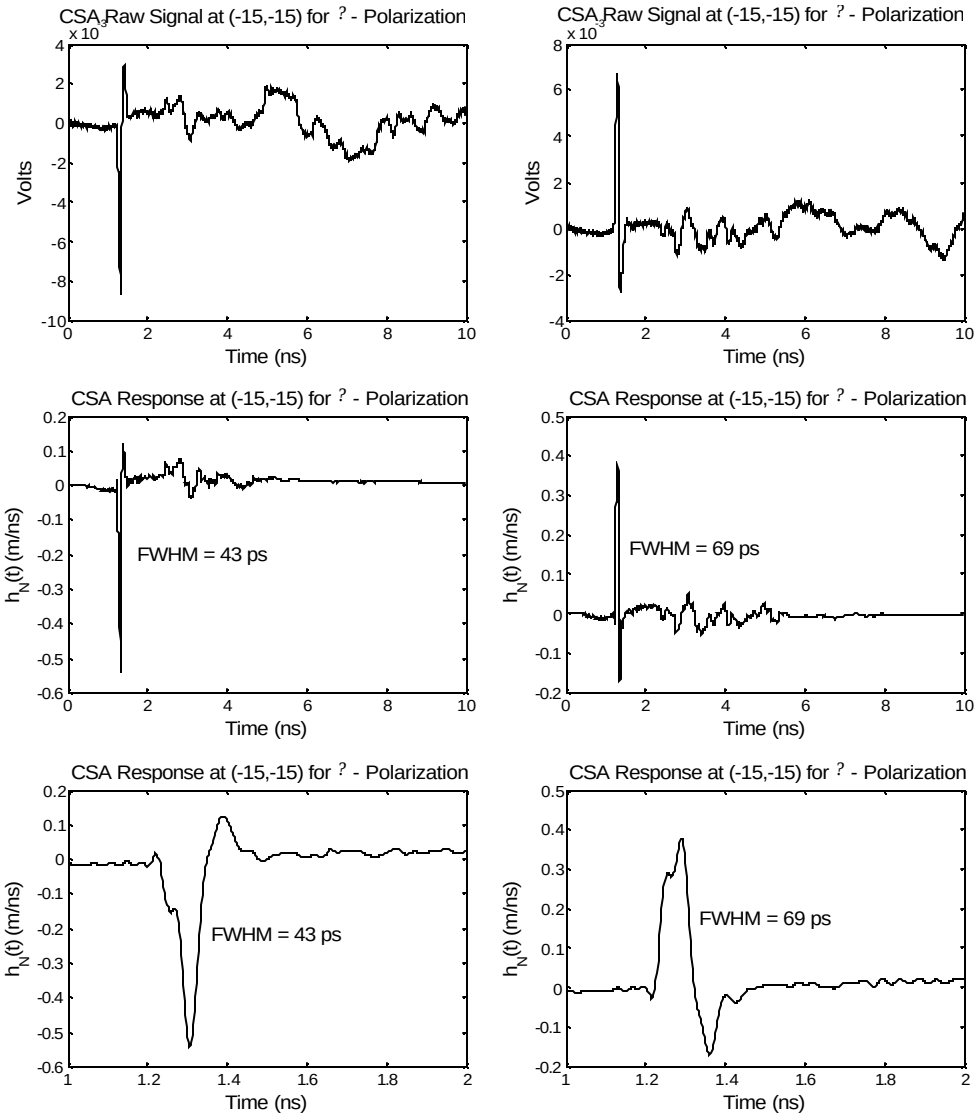

Figure 14. Impulse response of the open-slot CSA at orientation (−15,−15).

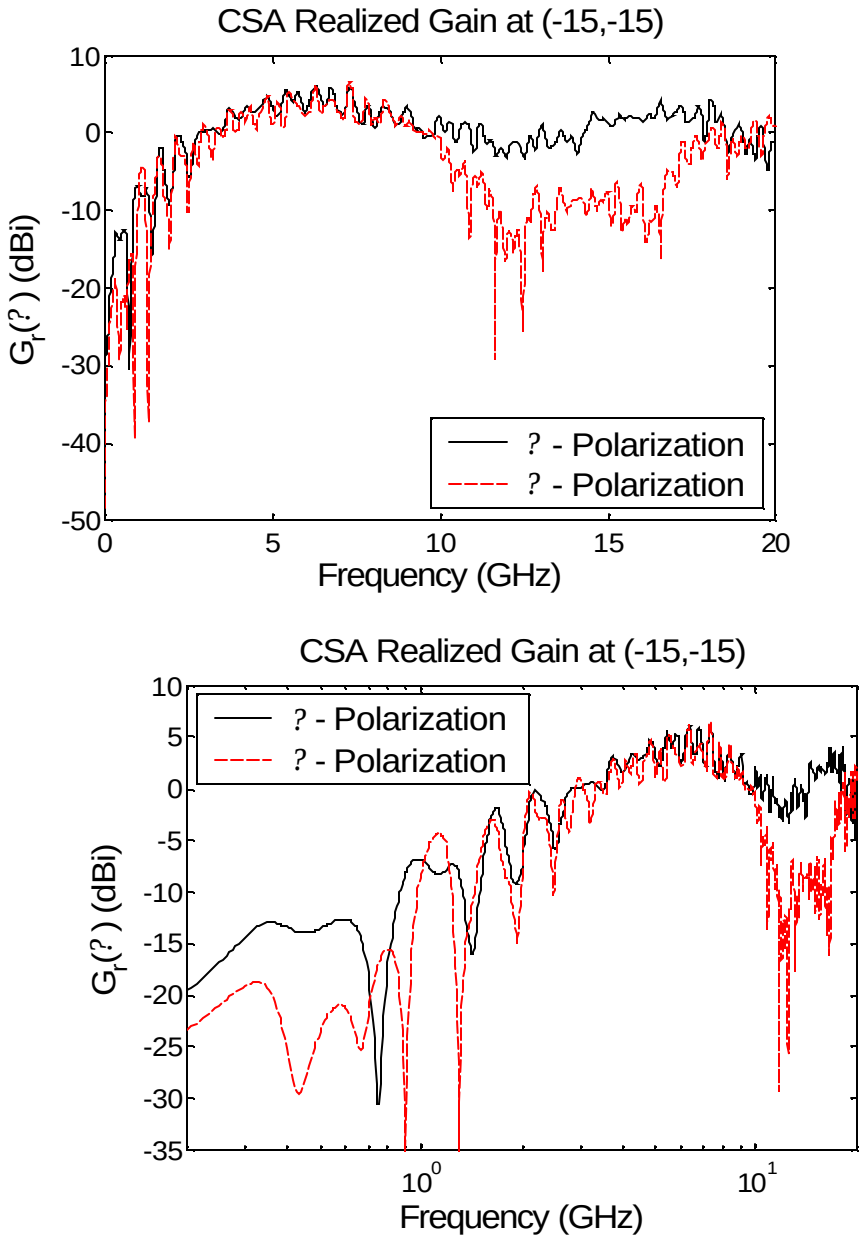

Figure 15. Realized gain of the open-slot CSA at orientation (−15,−15)

5. Other Antenna Concepts for Inflatable Wings

Finally, we consider a number of related antenna concepts that may find use on an aircraft with inflatable wings. The simplest concept is the Tapered Slot Antenna (TSA). An example of such a device is shown in Figure 16, along with a possible mounting method. The width of the slot may be tapered in either a linear or spline shape, and examples of each are shown in Figure 17. Results on these devices will be published in a forthcoming note.

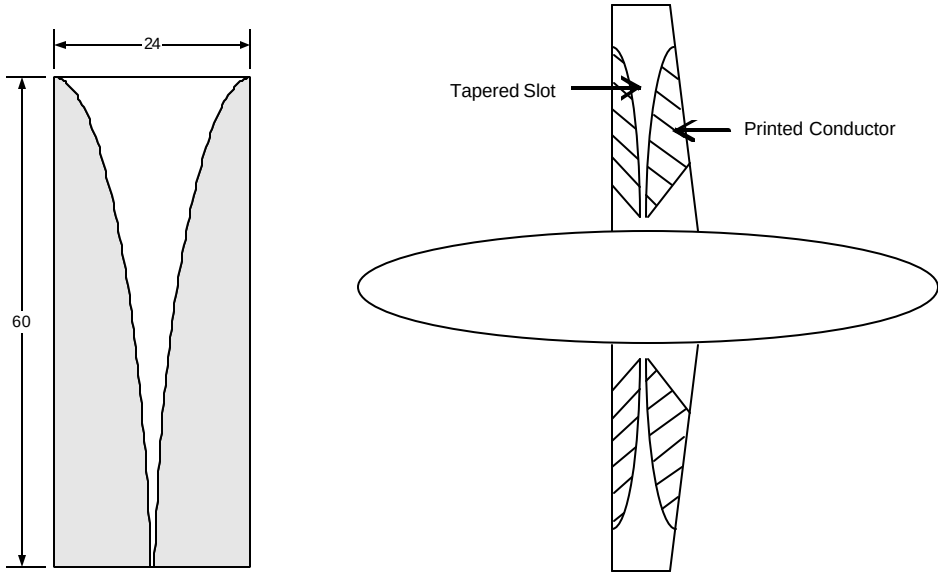

Figure 16. Full-scale tapered slot antenna (top, dimensions in inches), and a pair of tapered slot antennas printed on aircraft wings (bottom).

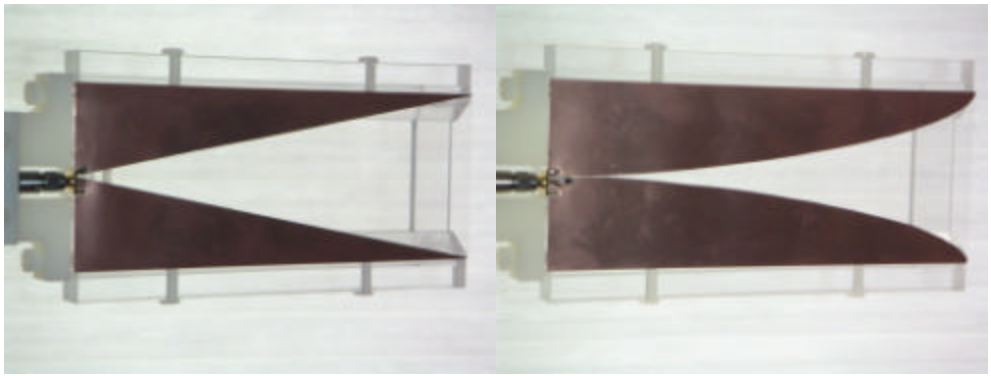

Figure 17. Copper-foil-tape-on-Mylar® linear-taper slot antenna (F/M LTSA, left) and spline-taper F/M STSA (right). Each antenna is mounted on an acrylic frame.

A number of other designs may be useful on inflatable wings on UAVs. The first of these is the four-strip pyramid, shown in Figure 18. When embedded into a wing this can be configured to receive either horizontal or vertical polarization. However, this design has the disadvantage of requiring access to the interior of the wing. It would be preferable to have a design that can be painted or printed onto the wing after it has been built.

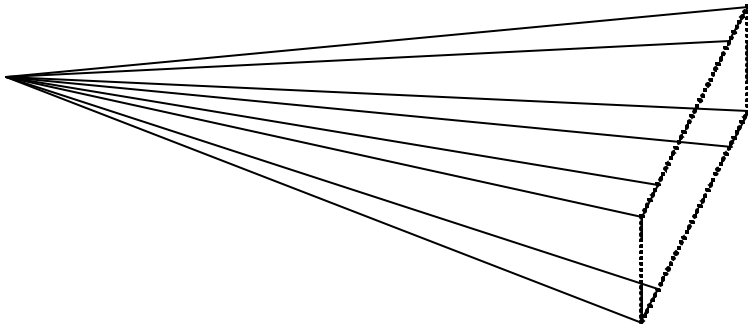

Figure 18. Four-strip pyramidal antenna.

The next configuration is the Maltese cross printed onto the underside of a wing as shown in Figure 19. This version receives both horizontal and vertical polarization. The component of vertical polarization is only that which is below the horizon. It should work well but it does not take advantage of the entire length of the wing to achieve the maximum possible response at low frequencies.

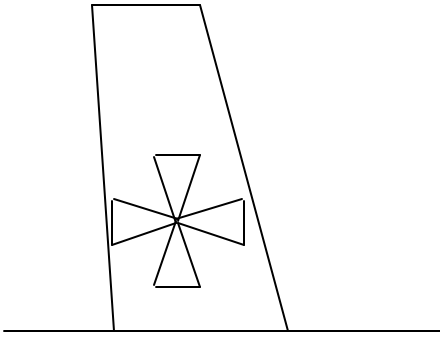

Figure 19. Maltese cross antenna.

To take better advantage of the wing size, one might use a bowtie antenna printed onto a dielectric wing, as shown in Figure 20.

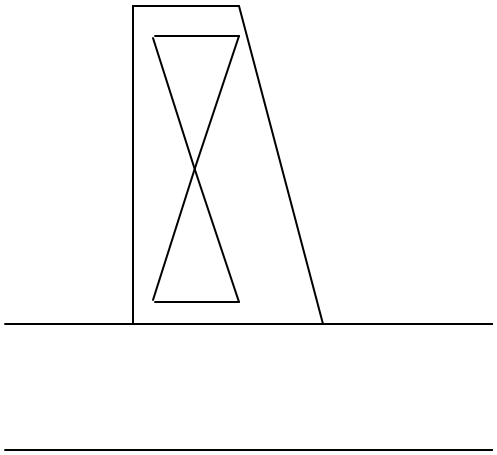

Figure 20. Bowtie antenna.

To take maximum advantage of the wing size, one might use a flat monocone against a conducting fuselage, as shown in Figure 21. This works if the wing is non-conducting and the fuselage is conducting. If the fuselage is dielectric, one might print a conductor onto the fuselage, as shown later in Figure 23.

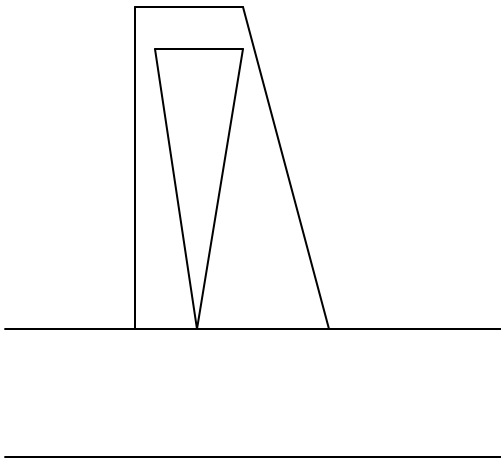

Figure 21. Flat monocone driven against a conducting fuselage.

An example of a dual polarization antenna is the dual polarization bowtie, shown in Figure 22. This consists of four triangular conducting strips mounted onto a dielectric wing located at the bottom of a fuselage. To drive the antenna for horizontal polarization we drive arms 1 and 3 against 2 and 4. To drive the antenna for vertical polarization we drive arms 1 and 2 against arms 3 and 4. As before this concept provides only the component of the vertical polarization that is below the wingtip.

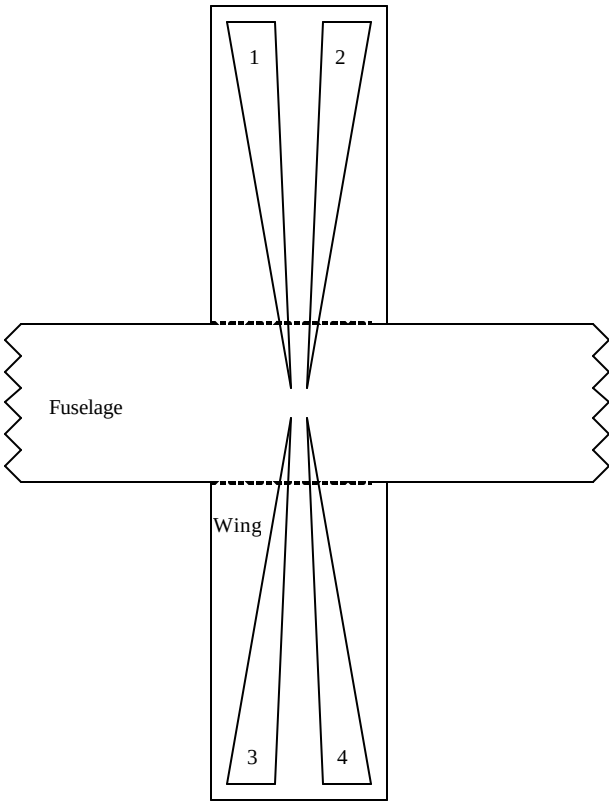

Figure 22. Dual polarization bowtie mounted onto the lower surface of a dielectric wing.

If both the wing and fuselage are dielectric a conformal horn could be realized by printing triangular patches onto the wing and fuselage as shown in Figure 23. We observe that the conformal horn is inherently a dual polarization device, though E and H plane responses may not be equally intense.

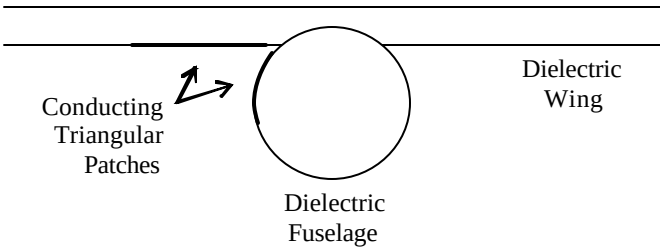

Figure 23. Use of UAV geometry to form a conformal horn.

Finally, we note that the optimal vertical polarization may be obtained by printing a conducting monopole onto the vertical stabilizer of the UAV as shown in Figure 24. This antenna can be driven against a conducting fuselage. If the fuselage is not conducting, a triangular patch can be printed onto it as shown in Figure 23 for the conformal horn.

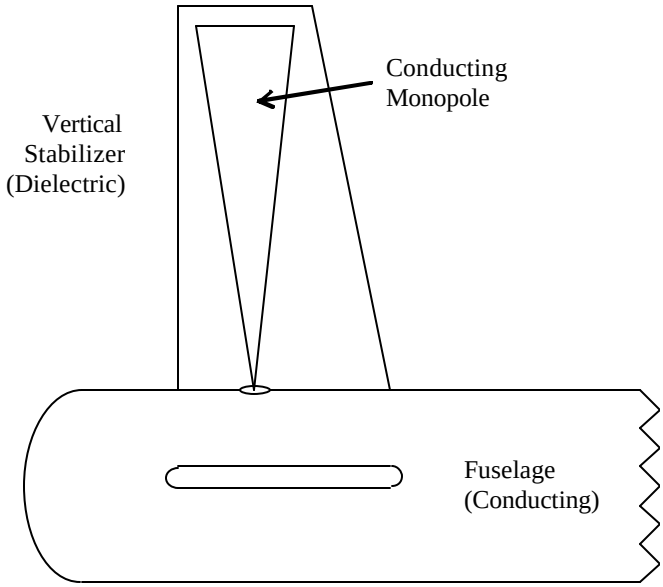

Figure 24. Vertical monopole mounted onto a dielectric vertical stabilizer.

6. Concluding Remarks

The CSA class of conformal UWB antenna introduced here appears to have potential for use as a vertically polarized radar receive antenna capable of being printed onto the wing of a UAV. Refinements in feed point design and slot shape and termination can be expected to reduce return loss and improve sensitivity to radiation reflected from ground targets.

We intended to design for a "typical" wing dimension of 1.52 m (5 ft.) in length by 0.91 m (2 ft.) in width, and our model was 1/8th this size. We observed a clean impulse response with FWHM of less than 70 ps. The realized gain was greater than 0 dBi over a frequency range of 4 to 12 GHz. In a full-scale design this would correspond to a bandwidth of 0.5 to 1.5 GHz. The return loss is higher than we would like over most of the frequency range.

Most of the CSA data we have presented here has been for the open-circuited configuration. In this configuration, we observe a strong vertical polarization at ± 17º below boresight in the vertical plane, and strong horizontal polarization at ± 15º to the left and right of boresight in the azimuthal plane. However, this second horizontal component is actually not helpful to the intended purpose. We speculate that shorting the end of the slots will reduce the unwanted horizontal component. One might treat the return loss by either tapering the slots or by adding a gradual resistive loading across the slot. It would be of interest to pursue this configuration further in future work.

Finally, we have sketched out a number of alternative antenna designs that may find use on an aircraft with inflatable wings. Many of these designs will be of interest and should be investigated further.

References

1 D. Cadogan, W. Graham, and T. Smith, "Inflatable and Rigidizable Wings for Unmanned Aerial Vehicles, published by AIAA, 2003, and available at http://www.ilcdover.com/products/aerospace_defense/supportfiles/AIAA2003-6630.pdf

2. C. E. Baum, Limited-Angle-of-Incidence and Limited-Time Magnetic Sensors, Sensor and Simulation Note 447, 18 April 2003.

3. E. G. Farr and C. E. Baum, Prepulse Associated with the TEM Feed of an Impulse Radiating Antenna, Sensor and Simulation Note 337, March 1992.

4. E. G. Farr, Optimizing the Feed Impedance of Impulse Radiating Antennas (Part 1: Reflector IRA's, Sensor and Simulation Note 354, January 1993.

DISTRIBUTION LIST

DTIC/OCP 8725 John J. Kingman Road, Suite 0944 Ft. Belvoir, VA 22060-6218	1 cy
AFRL/VSIL Kirtland AFB, NM 87117-5776	2 cys
AFRL/VSIH Kirtland AFB, NM 87117-5776	1 cy
Official Record Copy AFRL/DEHP/Lt Joe Broeckert	2 cys